Design Considerations for Low-Margin Elastic Optical Networks in the Nonlinear Regime

SEB J. SAVORY[1,*], ROBERT J. VINCENT[1], AND DAVID J. IVES[1]

[1] University of Cambridge, Department of Engineering, Electrical Engineering Division, 9 JJ Thomson Avenue, Cambridge, CB3 0FA, U.K.
[*] Corresponding author: sjs1001@cam.ac.uk

Compiled August 20, 2019

We demonstrate from a system design perspective, that nonlinearity can be exploited, to minimize the impact of system margins on the system performance, both for point-to-point links and elastic optical networks. A nonlinear interaction causes a 2 dB reduction in launch power to be reduced to <0.25 dB signal-to-noise ratio (SNR) penalty and likewise, a 2 dB peak-peak (pk-pk) perturbation to the output power of an optical amplifier incurs <0.25 dB SNR penalty (for 5, 10 and 20 spans). Extending this to a gain ripple of 1 dB pk-pk with an internode spacing of 5x80 km, 10x80 km and 20x80 km the penalty is 0.4 dB, 1.5 dB and 5.1 dB, respectively, with pre-emphasis reducing this to 0.01 dB, 0.3 dB and 1.2 dB respectively. In elastic optical networks we consider the nonlinear relationship between SNR, margin and the fraction of capacity available. We consider scaling internode distances of a 9-node German scale network (DT9) such that the initial network diameter increases from 1,120 km to 6,720 km (six-fold scaling). We generate 1,000 different topologies based on the scaled DT9 node locations to quantify the impact of margin. For the unscaled DT9 network a 3 dB margin results in, on average, a 21% reduction in network throughput, however when the internode spacing is increased six-fold to a continental scale network, the network throughput is reduced by 40%, on average, for the same 3 dB margin.

http://dx.doi.org/10.1364/jocn.XX.XXXXXX

1. INTRODUCTION

As optical networks are pushed to their limits there is a need to reduce the margins allocated in order to ensure an installed system operates satisfactorily over its lifetime[1]. Likewise as systems are pushed to their limits, elastic optical networks are pushed into the nonlinear regime, operating at the optimum launch power to maximize the available signal to noise ratio[2]. There is however an interaction between system perturbations and the nonlinear system response[3]. In this paper we will aim to highlight some of the key interactions that occur in nonlinear elastic optical fiber networks. One aspect is the interaction between the margins and the variation in system performance which we will discuss in the background section, before moving on to discussing the effect of moving to elastic optical networks where the data transmitted by a fixed symbol rate transceiver will varying according to the available signal-to-noise ratio (SNR). Following on from these introductory elements, we discuss two areas where the interaction between margins and performance warrants further discussion. The first of these is concerned with the effect of optical amplifier gain ripple on system performance, highlighting that through careful design in the nonlinear regime the impact of this is significantly minimized. The second concerns the impact of system margins on the throughput of a 9-node mesh network, exploring multiple scales and one thousand different options for connectivity. At the end of the paper we draw our conclusions.

2. EXPLOITING SYSTEM NONLINEARITIES

In general system nonlinearities are considered detrimental, for example in a transmission system the nonlinear Kerr effect limits the maximum signal to noise that can be achieved. Nonetheless from the perspective of design, nonlinearities can be exploited in order to minimize the effect of uncertainty as highlighted in Jim Morrison's seminal 1957 paper on the study of variability on engineering design[4]. In the context of an optical fiber communication system, numerous nonlinear relationships exist which from a design perspective can be exploited, in order to minimize the variability of unknown inputs on the resulting performance. To illustrate this concept, let us consider the SNR of a system, which for a nonlinear fiber transmission system is of the form[5]

$$SNR = \frac{P}{a + bP^3} \tag{1}$$

where a and b are constants that depend on the system configuration (a is proportional to the total linear noise and b gives an indication as to the strength of the fiber nonlinearity). Initially as

the power is increased the SNR increases linearly, but eventually the SNR decreases as the inverse square of the power. Between these two extremes a maximum signal to noise ratio denoted SNR_0 is observed at a power of P_0. If we define a normalized power $p = P/P_0$ then with a little algebra it is straightforward to show that $s = SNR/SNR_0$ being a normalized SNR is:

$$s = \frac{3p}{2+p^3} \tag{2}$$

The conventional interpretation of Fig.1, which plots the normalized SNR (s) as a function of the normalized power (p) is to observe that the nonlinearity of the fiber presents a considerable detriment to increasing the SNR by increasing the launch power, placing a limit on the maximum achievable SNR. While this is indeed true, from the perspective of robust systems design, this same nonlinearity can be exploited to minimize the impact on the system performance to variations in the performance of system components.

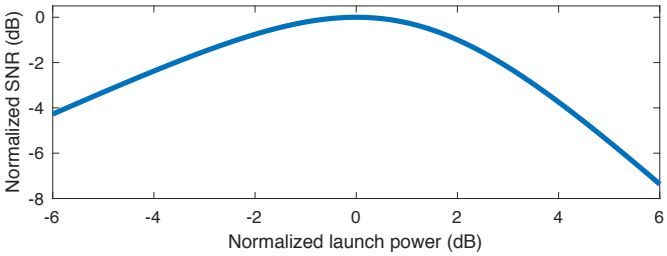

Fig. 1. Normalized SNR versus normalized launch power (normalized to the SNR at the optimum launch power and to the optimum launch power respectively)

In order to demonstrate the interaction of perturbations with the nonlinearity, we consider the case whereby the transmitted power decreases by 3 dB due to aging over its lifetime such that $P_{BoL}/P_{EoL} = 2$, where P_{BoL} is the launch power at the beginning of life (BoL) and P_{EoL} is the launch power at the end of life (EoL). If the corresponding normalized parameters are p_{BoL}, $p_{EoL} = p_{BoL}/2$, s_{BoL} and s_{EoL}, then as illustrated in Table 1 there is a solution such that $s_{BoL} = s_{EoL}$, with $p_{BoL} = +1.4$ dB.

p_{BoL} (dB)	s_{BoL} (dB)	p_{EoL}	s_{EoL} (dB)	ΔSNR (dB)
-3	-1.5	-6	-4.3	2.8
0	0	-3	-1.5	1.5
+3	-2.2	0	0	2.2
+1.4	-0.5	-1.6	-0.5	0

Table 1. Impact of provisioning with the nonlinear performance from Fig. 1 on SNR over life with a 3 dB degradation in power

Consequentially a 3 dB variation in power has been reduced to a 0.5 dB variation in the SNR highlighting improvement afforded by the nonlinearity with regards to the interaction between variations and the system performance. More generally if $p_{EoL} = p_{BoL}/M$ then $s_{BoL} = s_{EoL}$ for some optimum $\hat{p}_{BoL}$ is:

$$\hat{p}_{BoL} = \sqrt[3]{\frac{2M^2}{M+1}} \tag{3}$$

and corresponding optimal SNR is given by $\hat{s}$ being equally to $s_{BoL} = s_{EoL}$ which is given by

$$\hat{s} = \frac{3}{2}\frac{\sqrt[3]{2M^2(M+1)^2}}{M^2+M+1} \tag{4}$$

As can be seen in Fig. 2 if the optimum bias points are used such that $p_{BoL} = \hat{p}_{BoL}$, the impact of the power variation in decibels given by $10\log_{10}(M)$ on the SNR penalty is significantly less than might have been expected from a linear analysis[1].

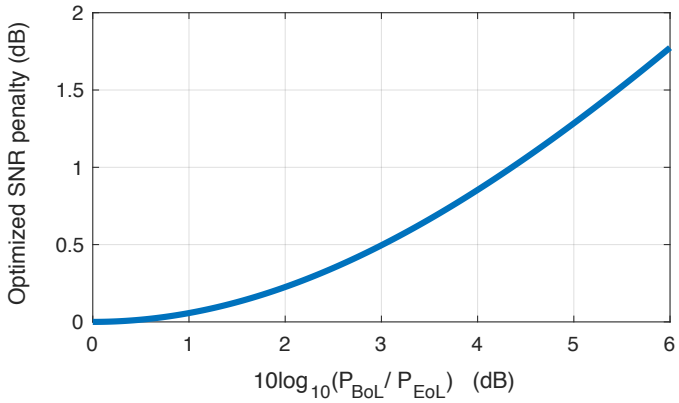

Fig. 2. Optimized SNR penalty versus power variation over life $10\log(P_{BoL}/P_{EoL}) = 10\log_{10}(M)$ at the optimal $\hat{p}_{BoL}$ such that $s_{EoL} = s_{BoL}$ has solution $\hat{s}$

The aim of this introductory section is to highlight, that while nonlinearities are detrimental in terms of overall performance from a design perspective there are significant benefits in terms of reducing the variation of performance in the presence of uncertainty.

3. EXPLOITING NONLINEARITIES TO REDUCE THE IMPACT AMPLIFIER OUTPUT POWER UNCERTAINTY

To quantify issues due to margins associated with optical amplifiers, we first consider the unperturbed ideal case in the nonlinear regime. For this unperturbed case we calculate the received SNR based on the model described in the Appendix with the parameters of table 6 and plot in Fig. 3 the worst case SNR across all WDM channels as a function of the uniform launch power per channel. As expected a 3 dB reduction in SNR is observed each time the number of spans are doubled, with an optimum launch power of approximately -1.3 dBm per channel.

In order to investigate the interaction between nonlinearity and margins we first consider the case where the launch powers are perturbed by a fixed multiplier. Such an error may occur due to inaccurate power monitors or VOA settings. Fig. 4 shows the minimum SNR across all channels as a function of the intended launch power for different power perturbations from 0 to 1 dB, with 1 dB corresponding to a ± 1 dB perturbation to the output power, i.e. 2 dB peak-peak (pk-pk). It can be seen that the received SNR shows a spread of $\approx$1 dB in the linear transmission regime, $\approx$2 dB in the highly nonlinear regime but at the optimal launch power show a much reduced spread of $\approx$0.25 dB. Fig. 5 shows the SNR penalty as a function of the power perturbation at the optimum flat launch power. The SNR penalty is independent of the number of transmission spans.

[1]If we define $M_{dB} = 10\log_{10}(M)$ then for $0 \le M_{dB} \le 3$ the SNR penalty ΔSNR_{dB} in decibels varies as $\Delta SNR_{dB} = \ln(10)M_{dB}^2/40$

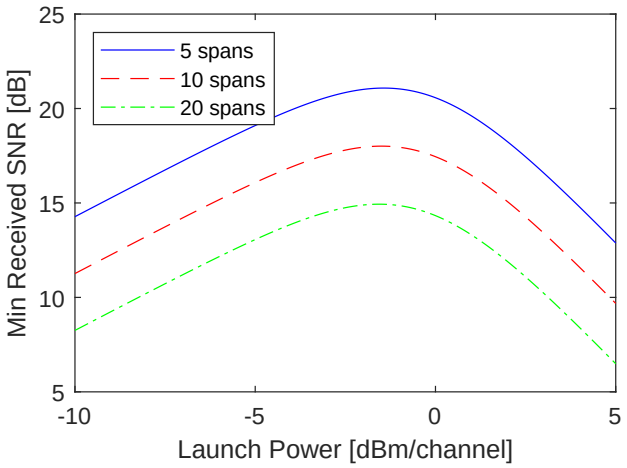

Fig. 3. Minimum channel SNR vs launch power for a spectrally flat launch power and ideal ripple free EDFAs. 5, 10 and 20 span transmission are shown.

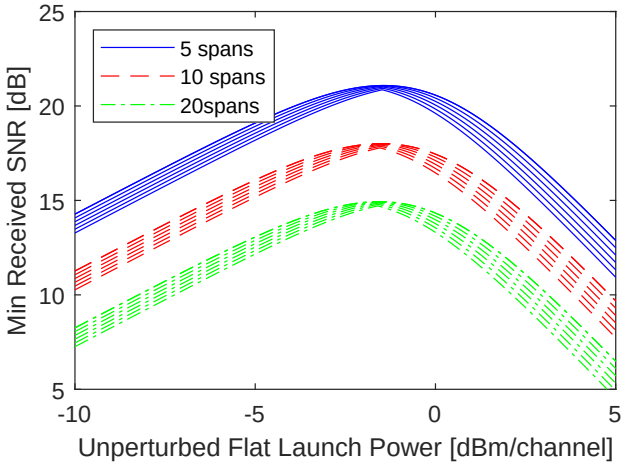

Fig. 4. Minimum channel SNR vs launch power for a spectrally flat launch power. The launch powers are perturbed by 0 to 1 dB to reflect the uncertainty of equipment. 5, 10 and 20 span transmission are shown.

4. EXPLOITING NONLINEARITIES TO REDUCE THE IMPACT OF EDFA GAIN RIPPLE ON TRANSMISSION PERFORMANCE

We also wish to understand the effect of EDFA gain ripple on the minimum transmission performance across channels in the nonlinear regime and investigate launch power optimization to mitigate the effect of channel power excursions. Sun et al. considered only linear transmission and a spectrally flat launch power and showed the OSNR penalty versus number of spans transmitted for different EDFA gain ripple[6]. The penalty rises slightly faster than linear in terms of ripple times spans product. While Barboza et al. looked at adapting the operating conditions of all the EDFA within a link to minimize the transmission penalty by operating the EDFA in a good gain ripple and noise figure regime[7]. The gain ripple can be mitigated by pre–emphasis of the launch powers as developed by Forghieri et al. for the linear transmission regime[8]. Here we consider

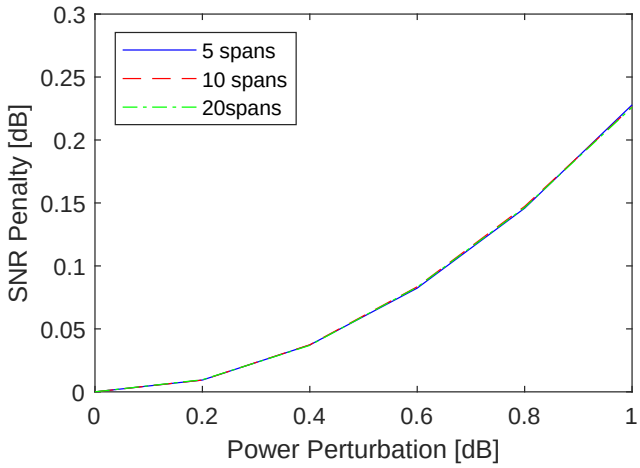

Fig. 5. SNR penalty vs power perturbation for a spectrally flat launch power. 5, 10 and 20 span transmission are shown.

the nonlinear transmission regime where modern optical coherent communications systems operate. We choose to perform a link level optimization maximizing the minimum SNR of all channels and effectively giving all channels the same SNR degradation through the link. This approach separates the physical layer link optimization from the network routing and spectrum assignment. The result will be sub-optimal from a network perspective but more tractable than a global optimization of power, routing and spectrum assignment.

For a given EDFA ripple, $2A$, the SNR of all the channels at the output after N spans was calculated assuming a launch power into the 1st span given by 1) a flat spectral power across all channels optimized to maximize the lowest SNR, and 2) individually optimized power for each channel to maximize the lowest SNR and effectively maximize a flat constant SNR of all the output channels. For the case 1) the launch power was optimized by an enumerated search while for case 2) the individual channel powers were optimized by gradient descent to achieve a target SNR and this target SNR was maximized by an incremental search. The gradient of SNR with channel power used is given by

$$Grd_w = \text{sign}\left[\frac{1}{SNR_w^{ASE}} - 2\frac{1}{SNR_w^{SCI}}\right] \quad \textbf{(5)}$$

and the launch power iterative update given by

$$P_{w,1} = P_{w,1}\left(\frac{SNR^{target}}{SNR_w}\right)^{Grd_w} \quad \textbf{(6)}$$

where SNR^{target} is the target SNR for the launch power optimization and this itself was maximized by an incremental search. Equation Eq. (6) describes a simple gradient descent optimization in the log domain where convergence has been explored by other authors[9]. To ensure convergence to the lowest launch power that achieves the target SNR the launch power iteration was initialized with a low power and post convergence Grd_w was confirmed as 1 for all channels w.

Fig. 6 shows two examples of this pre–emphasis, for an ideal gain flat EDFA and for an EDFA gain profile with pk-pk ripple of 1 dB. The optimum launch power spectrum to maximize the lowest SNR along with the received power spectrum and the

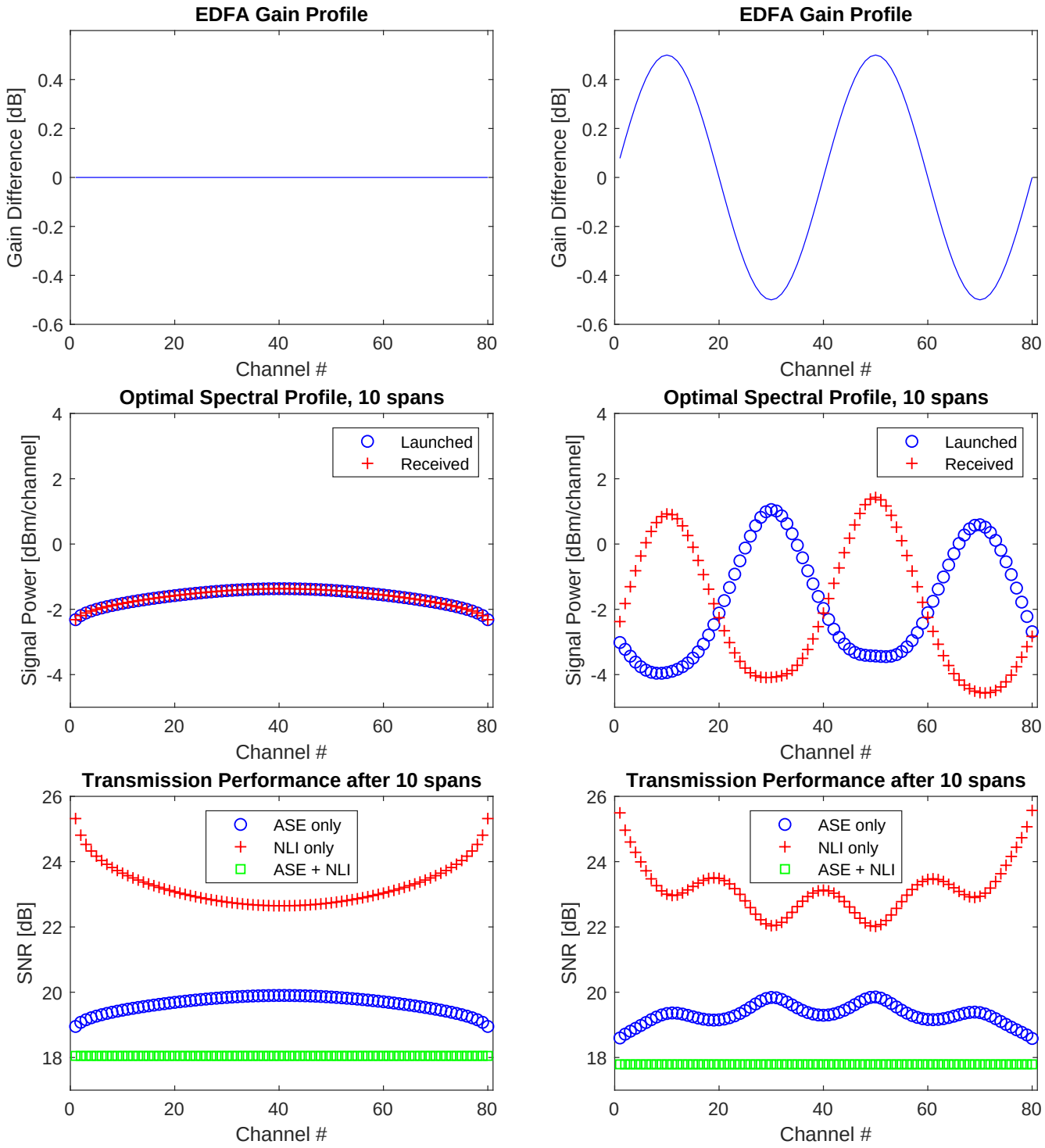

Fig. 6. Illustration for 10 span transmission with EDFAs having ideal flat gain (left) and gain with a pk-pk ripple of 1 dB (right). Individual launch powers optimized to maximize the lowest SNR.

SNR performance, the linear SNR, nonlinear SNR and the total SNR for transmission through 10 spans are also shown.

Fig. 7 shows the minimum received SNR across channels as a function of the pk-pk EDFA gain ripple for different numbers of transmission spans. For the optimum spectrally flat launch power the minimum SNR decreases with increasing ripple times spans product. However this decrease is slower than that expected from the signal power excursions since the nonlinear transmission mitigates the effect on the SNR. For individually optimized launch powers, the pre–emphasis of the launch power attempts to mitigate the power excursions to give a spectrally flat transmission performance as illustrate in Fig. 6. The reduction of minimum SNR with EDFA gain ripple increases more quickly than linear with ripple times number of spans, but this means for a small ripple or limited number of spans the effect can be almost completely mitigated.

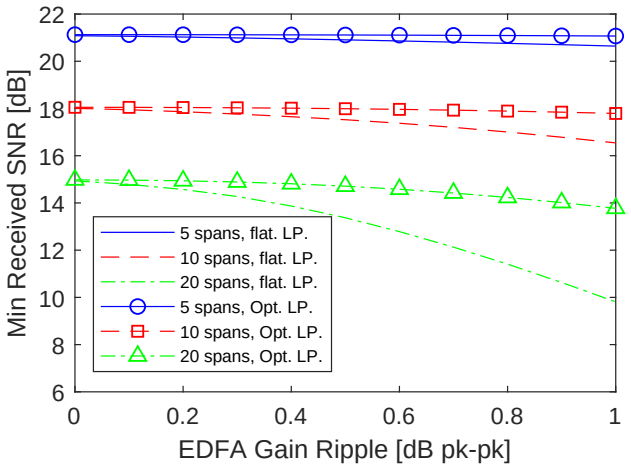

Fig. 7. Minimum channel SNR vs EDFA gain ripple for 5, 10 and 20 span transmission. The minimum channel SNR for an optimum spectrally flat launch power and for individually optimized launch powers are shown.

EDFA gain ripple [pk-pk dB]	0.0	0.5	1.0
SNR penalty after 5 × 80 km [dB]	0.0	0.2	0.4
SNR penalty after 10 × 80 km [dB]	0.0	0.5	1.5
SNR penalty after 20 × 80 km [dB]	0.0	1.6	5.1

Table 2. SNR penalty caused by EDFA gain ripple for a spectrally flat launch power.

EDFA gain ripple [pk-pk dB]	0.0	0.5	1.0
SNR penalty after 5 × 80 km [dB]	0.0	0.0	0.0
SNR penalty after 10 × 80 km [dB]	0.0	0.0	0.3
SNR penalty after 20 × 80 km [dB]	0.0	0.3	1.2

Table 3. SNR penalty caused by EDFA gain ripple for an individual channel optimized launch power.

Table 2 and table 3 show the SNR penalty for different numbers of transmitted spans and for different EDFA gain ripple under a spectrally flat launch power and for individual channel optimized launch powers. These shows that for a EDFA with 1 dB of pk-pk ripple a link of 20 spans would have an SNR penalty of over 5 dB if a spectrally flat launch power is employed. This penalty can be mitigated and reduced to 1.2 dB by pre-emphasizing the launch power. The penalty appears to grow quadratically with number of spans limiting the maximum number of spans for pre-emphasis. In metropolitan networks with ROADM nodes spaced by less than 10 spans, 800 km, pre–emphasing the launch power following each ROADM node reduces the link penalty to <0.3 dB. Thus even for a multi-hop route up to 2500 km, SNR penalties of <1 dB can be expected across channels. For smaller metro networks larger EDFA gain ripple can be accepted whilst maintaining a <1 dB penalty.

In the preceeding analysis the wavelength dependence of the fibre attenuation and stimulated Raman scattering (SRS)[10–12] have been ignored. These effects will slightly tilt the received power spectrum across the transmission band and as a secondary effect alter the strength of NLI generation. Assuming the EDFA gain tilt can be adjusted to compensate this received power tilt the power deviations will not accumulate in subsequent spans. Pre-emphasize of the launch power can be used to mitigate the received power tilt[10, 12] and the EDFA noise figure variations both will lead to a penalty, this is left for further study.

5. EXPLOITING THE NONLINEARITY OF THE SHANNON CAPACITY RELATIONSHIP

Thus far we have focused on the nonlinearity associated with the Kerr effect in an optical fiber. In the subsequent sections we wish to exploit a different nonlinear relationship, namely the logarithmic relationship between SNR and the Shannon capacity, as approached by a transceiver in an elastic optical network. Let us begin by considering the idealized case such that the capacity per polarization is given by the Shannon capacity for the additive white Gaussian noise channel[13]

$$C = B\log_2(1+SNR) \tag{7}$$

where B is the bandwidth and SNR is the signal to noise ratio. If we apply a system margin M which in decibels is denoted by $M_{dB} = 10\log_{10}(M)$ then we can write the capacity as a function of margin M such that

$$C(M) = B\log_2\left(1+\frac{SNR}{M}\right) \tag{8}$$

Hence we can deduce that the fraction of the capacity available with a margin M is given by

$$\frac{C(M)}{C(1)} = \frac{\log_2\left(1+\frac{SNR}{M}\right)}{\log_2\left(1+SNR\right)} \tag{9}$$

If we define $SNR_{dB} = 10\log_{10}(SNR)$ then $C(M_{dB})$, the capacity as function of the margin in decibels M_{dB} is

$$\frac{C(M_{dB})}{C(0)} = \frac{\log_2\left(1+\frac{10^{SNR_{dB}/10}}{10^{M_{dB}/10}}\right)}{\log_2\left(1+10^{SNR_{dB}/10}\right)} \tag{10}$$

As illustrated in Fig. 8 it can be seen that for systems operating with high SNR the impact on the overall capacity is

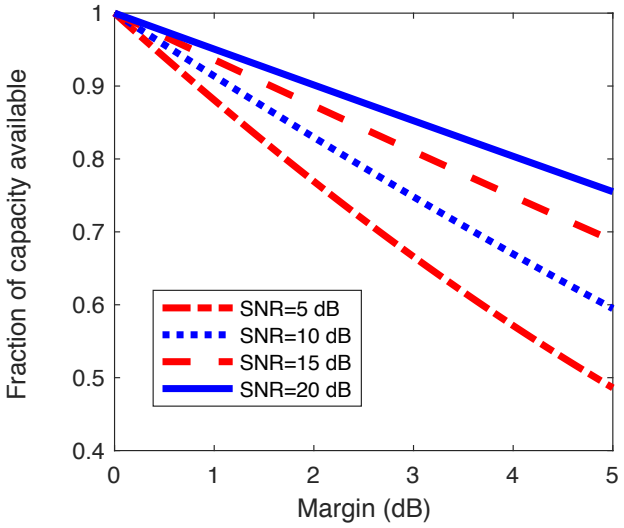

Fig. 8. Effect of margin on the fraction of capacity available for a range of SNR values

Format	Min SNR (dB)	Data Rate (Gb/s)	Reach (# spans)
PM–BPSK	3.7	50	240
PM–QPSK	6.7	100	123
PM–8QAM	10.8	150	49
PM–16QAM	13.2	200	29
PM–32QAM	16.2	250	14
PM–64QAM	19.0	300	7
PM–128QAM	21.8	350	4
PM–256QAM	24.7	400	2
PM–512QAM	27.4	450	1

Table 4. Minimum SNR required for the modulation formats used with the post–FEC data rate and reach (with 1 amplifier per span)

significantly reduced to lower SNR systems. In order to provide further insight if we assume $SNR \gg 1$ and noting that $10 \times \log_{10}(2) \approx 3$ we can write

$$C(M_{dB}) \approx \frac{B}{3}\left(SNR_{dB} - M_{dB}\right) \tag{11}$$

therefore

$$\frac{C(M_{dB})}{C(0)} \approx 1 - \frac{M_{dB}}{SNR_{dB}} \tag{12}$$

This indicates that the throughput relative to the case for 0 dB margin falls off approximately linearly with the margin M_{dB} given in decibels, in agreement with that observed in Fig. 8. As we shall see in Section B this approximately linear relationship is observed for the network throughput albeit the SNR_{dB} takes into account the 'effective SNR' for the network when using practical modulation formats.

6. QUANTIFYING THE RELATIONSHIP BETWEEN NETWORK MARGIN AND CAPACITY

A. Simulation Parameters

In the following, we use the modelling procedure from [2] which we outline here for completeness. Transceivers are assumed to be capable of high order modulation formats with the required SNR for each given in Table 4. This assumes symbols are only mistaken for their nearest neighbours and that the forward error correction is capable of correcting a 1.5 % BER — we use a hard–decision staircase BCH code with 20 % overhead, although similar performance can be achieved with soft–decision. From this we see that a 3 dB margin will move most lightpaths to a lower order modulation format. The absolute effect is the same, a 50G reduction in bandwidth, but the transition from QPSK to BPSK is a 50 % reduction whilst 512–QAM to 256–QAM results in only a 11 % reduction in bandwidth.

To estimate QoT, we use the Gaussian Noise model with coherent SCI and incoherent XCI whilst neglecting FWM. This is a simplified version of the model detailed in the Appendix where each lightpath has the same launch power and amplifiers are flat across the C–band. If the launch power is the same for every transceiver we should choose the optimum however this is ambiguous because transmissions of different lengths have different NLI due to coherent SCI. Fortunately, from Fig. 3, we see that the optimum power is similar across a range of transmission distances with these assumptions. This allows us to use a single launch power across all lightpaths on any network without sacrificing much performance. To this end, we found the optimum launch power for a single span and used this optimum power for every transceiver on every network considered. The SNR of a single span is:

$$\text{SNR} = \frac{P}{N_{\text{ASE}} + P^3 \sum_{w' \in \{1..W\}} X_{ww'}}, \tag{13}$$

where the nonlinear term is taken from equation Eq. (26) with the number of spans, N, set to 1. Differentiation with respect to P gives the optimum launch power as

$$P_{\text{opt}} = \sqrt[3]{\frac{N_{\text{ASE}}}{2\sum_{w' \in \{1..W\}} X_{ww'}}}, \tag{14}$$

which gives a result of 0.74 mW or −1.3 dBm. This achieves the optimum SNR to within 0.1 dB for a fully loaded link of any transmission distance.[2]

B. Effects of Margin on a Variety of Topologies

To find the capacity of a network — defined here as the maximum traffic possible subject to uniform traffic between nodes — we must combine QoT estimation, see above, with routing and spectrum assignment [14]. For each request, this entails finding a path connecting the relevant nodes in combination with a wavelength that is unused along entirety of this path; this {path,wavelength} tuple is known as a lightpath. A trivial problem for a single lightpath, the complexity of RSA increases rapidly when we attempt to assign many lightpaths at once with each one 'competing' for resources; indeed the problem is analogous to graph coloring and is therefore NP–hard [15]. To make

[2]The optimum power for a fully loaded 240 span link, the maximum reach of BPSK, is −1.8 dBm which results in a 0.07 dB SNR improvement over the value we use. We feel this difference is small enough to warrant the significant decrease in complexity gained by having a single output power for every transceiver.

the problem tractable, even on large networks, lightpaths can be assigned sequentially rather than all at once. This obviously introduces the possibility of arriving at a sub–optimal solution however this can be mitigated with a forward looking RSA strategy [16]. We use the the FF–kSP algorithm with the number of route options k set to 5 — further details found in [17].

A test topology, DT9, is shown in Fig. 9. Link lengths were calculated using a great circle distance adjusted to a realistic fibre distance in accordance with [18]. We shall compare the effect of network margin by scaling this topology such that the connectivity stays the same but the absolute distances between nodes changes. The diameter, i.e. the longest shortest path, on DT9 is 1,120 km or 14 spans. From Table 4 we see that if we were using basic shortest path routing, all lightpaths would be capable of 32QAM or above. By comparison, we would need to scale DT9 to approximately 1:6, i.e. 1 km $\mapsto$ 6 km, to make it a similar size to NSFnet.

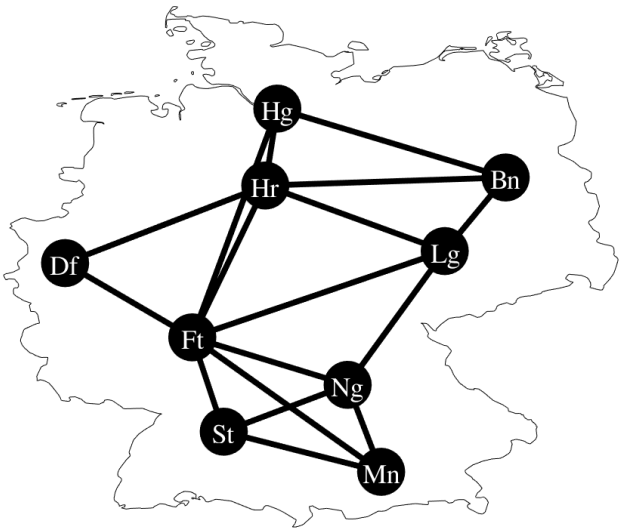

Fig. 9. Topology of DT9 within Germany [19]. While links are shown as straight lines they are assumed to deviate somewhat due to geography and are therefore slightly longer, as per [18].

We plot the effect of increasing network margin on DT9 in Fig. 10 in addition to the effect on the same topology scaled to larger sizes of 1:2, 1:4, and 1:6, with diameters of 2,240 km, 4,480 km, and 6,720 km, respectively. This allows us to compare networks in the regime of 32 QAM and above, for the true scale or 1:1, and an identical topology using QPSK and above. We can see that, as expected, an increase in network margin results in a larger proportional reduction in throughput for the larger topologies. Indeed, a 5 dB margin on the original topology is roughly equivalent to a 3 dB margin on the same topology with 6 times longer links. We fit data with a single variable, a, in the form $y = 1 - ax$. This results in a reasonable approximation although the overall trend is not linear, indeed when the margin increases to the point at which even BPSK is not achievable on the longest paths the throughput will crash to almost zero. This happens with the largest network, 1:6, with a 5 dB margin: this data point is not seen in the figure because the maximally separated node pair could not be connected, violating the uniform traffic requirement almost immediately. An important note is that with very low margin, i.e. 0–2 dB, the difference is minimal. This contrasts with the clear difference, especially between 1:1 and 1:6, when using more significant margins such as 3–5 dB. Here we see a performance penalty of using a given margin that is over 10 percentage points lower on a large network. Despite its limitations, the gradient of the linear fit, a, gives the mean percentage penalty per dB of margin for the 1:1, 1:2, 1:4, and 1:6 scales this value was 6.58±0.05, 9.10±0.05, 9.79±0.06, and 12.24±0.04, respectively. To test the goodness–of–fit we use the standard reduced chi–squared test where a value of $\chi^2_{\text{red}} \approx 1$ indicates the fit is representative, lower values indicate over–fitting, and higher values indicate a poor model for the data. From this we can take the fits for 1:1 and 1:2 as representative however the larger χ^2_{red} for the fits for 1:4 and 1:6 indicate that the linear fit, and hence the gradient, should be used with caution. This is especially true for 1:6 because the fit does not include the data for 5dB margin.

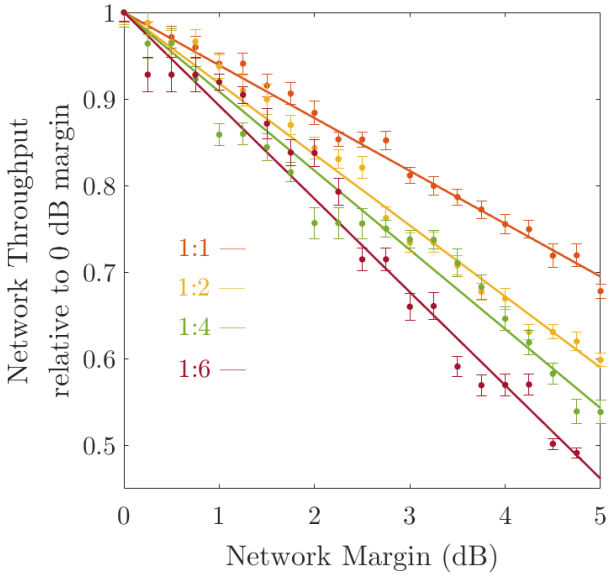

Fig. 10. Effect of margin on the throughput on the DT9 topology illustrated in Fig. 9 scaled from 1:1 up to 1:6 for a diameter ranging from 1,120 to 6,720 km. We see that for the scaled DT9 topologies, a larger network is more affected by increasing margin, especially for 3 dB and up. The linear fits forced the intercept to 1 and resulted in χ^2_{red} of 0.8, 1.6, 3.4, and 4.3 for scales 1:1, 1:2, 1:4, and 1:6, respectively.

We can extend this approach to the set of 1,000 networks, introduced in [16], generated with a genetic algorithm that selected the set of links connecting the nodes in Fig. 9 that minimized the product of graph diameter and total fibre length. This approach provided typical network topologies in which each link either connected nodes or reduced the maximum distance between nodes. Some example topologies are given in Fig. 11.

For each network topology we can generate an identical plot to that of Fig. 10. For clarity, we shall show the effect of a given margin on a range of topologies in the form of a histogram of the mean throughput relative to the optimum, i.e. with 0 dB margin; this can be seen in Fig. 12. We show the relative performance with margins from 1 to 5 dB and see that the effect of margin varies with both topology and scale. Different topologies can behave quite similarly, for instance 1:1 with 3 dB margin with 79.5 ± 0.7 % performance, whereas in other cases, say 1:6 with 2 dB margin with 79 ± 4 %, the effect ranges about 20 percent-

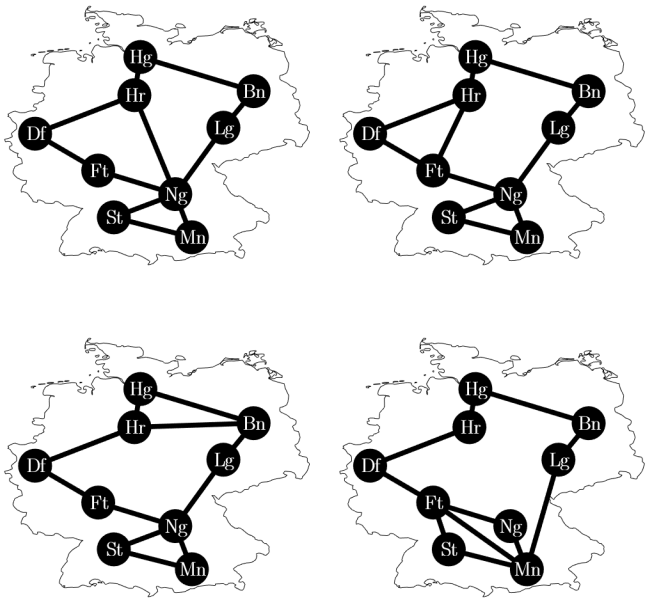

Fig. 11. Example topologies from the DT9TEST set of networks based on the node locations of DT9 in Fig. 9. Network ID numbers are 1, 10, 100, and 1,000, for the top–left, top–right, bottom–left, and bottom–right topologies, respectively.

age points different from the best– to worst–case. This is to be expected because we do not know which combination of lightpaths dictate performance for each network and each of these lightpaths will have different overheads and hence will not react to a given margin in the same way. This creates significant uncertainty when generalizing between multiple topologies even when those topologies are similar in some particular metrics.

The effect of margin on different scales behaves broadly in line with what we outlined above, namely that larger networks are more effected by a given margin, however the effect is not as consistent as its theoretical underpinnings might suggest. We see that a larger margin produces a larger performance penalty in most cases, although there is significant overlap especially when the difference between margins is just 1 dB. The more interesting result is the comparison between topologies of different scales. We see in Table 5 that the performance on 1:1 with a 5 dB system margin results in a smaller penalty than the networks scaled to 1:6 with a 3 dB margin. We also see that as we are using a relative metric we expect small differences with 1 dB margin but significant differences with large margins such as 5 dB.

This suggests two clear design rules: first, utilising more complicated modulation formats that take advantage of high SNR lightpaths allows a network operator to run a higher margin with less impact on network traffic. And second, when operating in lower SNR regimes, i.e. on larger networks, closer attention must be paid to optimizing performance. This follows because a reasonable operating margin, such as 3 dB, is likely to cost perhaps 40 % of network capacity on a network the size of the USA compared to just 20 % on a network the size of Germany.

7. CONCLUSIONS

We have investigated the relationship between system margin and performance for elastic optical networks operating in the nonlinear regime. Two areas were considered, the margins associated with cascaded optical amplifiers and also the throughput of an elastic optical network as a function of margin.

	Margin		
Scale	1 dB	3 dB	5 dB
1:1	93 ± 1	79 ± 1	65 ± 1
1:2	90 ± 2	69 ± 2	58 ± 1
1:4	87 ± 3	71 ± 3	50 ± 2
1:6	87 ± 2	60 ± 2	N/A

Table 5. Mean Performance on DT9TEST networks for different length scales and margins (% capacity relative to zero margin performance)

For the case of cascaded optical amplifiers with uncertainty in the output power of the optical amplifier we concluded that nonlinearity offered a significant advantage, reducing a 1 dB penalty over 5, 10 and 20 spans to less than 0.25 dB variation in received SNR. For the case of gain ripple, assuming gain equalization at network nodes we concluded that the scale of the network has a significant impact on the resulting penalty, with a 1 dB peak-peak gain ripple the penalty being 0.4 dB, 1.5 dB and 5.1 dB for 5x80 km, 10x80 km and 20x80 km respectively. This penalty can be significantly reduced by applying pre–emphasis to the launch powers, such that after 5x80 km there is a negligible penalty (0.01 dB), increasing to 0.3 dB and 1.2 dB for 10 and 20 spans respectively. This leads us to conclude that metropolitan scale networks are inherently more robust than long-haul scale networks to system margins.

A similar conclusion regarding the relative robustness of metropolitan scale networks compared to long-haul scale networks is also drawn when investigating the impact of system margin on network throughput. For example in the DT9 network, when the network is not scaled and so covered Germany with a 3 dB margin the capacity is 79% whereas when the internode spacing is increased by a factor of six (corresponding to a continental scale network) the capacity reduces to 60% due to the 3 dB margin.

APPENDIX

We assume that all sources of noise can be modeled by Gaussian noise and as such the overall SNR for a link is given by

$$SNR = \frac{P}{P_{ASE} + P_{NLI}} \tag{15}$$

where P is the signal power, P_{ASE} is the ASE noise power and P_{NLI} is the nonlinear interference noise, and all noise powers are measured within the receiver matched filter bandwidth. We also assume here that the transceiver noise sources are negligible.

In this work to assess the effect of amplifier gain ripple, the SNR model is extended to allow different launch powers for each channel into each span along the light path. We use a model based on the GN model [20] with uniform span lengths of 80 km and system parameters as described in Table 6. We assume each fiber span is followed by an EDFA to compensate for the fiber loss. Nonlinearity from self–channel interference (SCI) is assumed to be coherent whilst cross–channel interference (XCI)

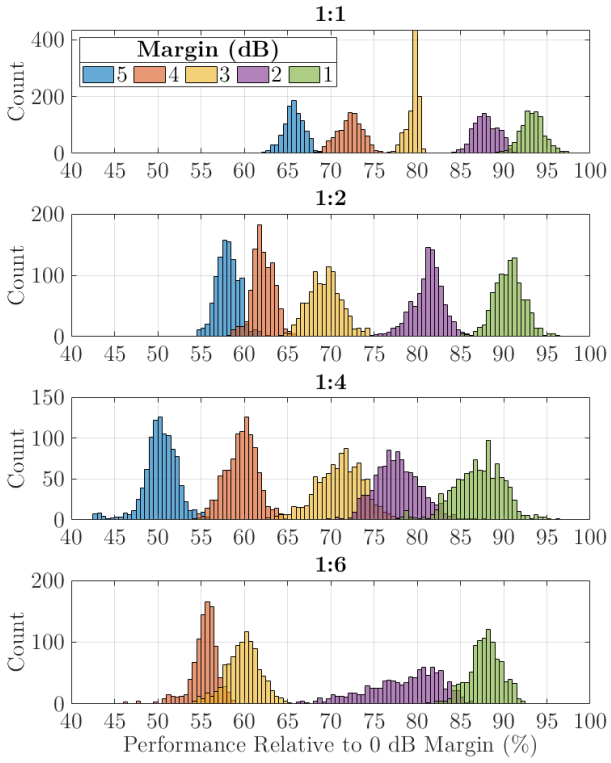

Fig. 12. Relative network throughput on the 1,000 DT9TEST networks scaled to 1:x whilst maintaining their topological structure for various margins. Data for a 5 dB margin on networks scaled to 1:6, i.e. equivalent size to NSFnet, is not shown because the longest lightpaths on many networks where unable to achieve even BPSK subject to Table 4 which we deem an unrealistic operating scenario.

is assumed incoherent; multi–channel interference is negligible due to relativity large guardbands.

Observations of ten similar gain flattened EDFAs in our laboratory show a pk-pk gain ripple of 0.8 dB across the C–band while the gain variation between EDFAs was less than 0.3 dB pk–pk across at a single channel. This suggests that for a single EDFA design the gain ripple is highly correlated between EDFAs. We thus model all the EDFAs as having an average gain equal to the span loss, $10^{(\alpha L)/10}$, with similar gain ripple, ΔG [dB], described by the following heuristic

$$\Delta G_w = A \sin\left[4\pi \frac{w}{W}\right] \tag{16}$$

where w is the DWDM channel number, $w \in 1 \ldots W$ and $2A$ is the peak to peak gain ripple. The choice of two ripple cycles across the C-band was influenced both by our observations of ten gain flattened EDFAs and to avoid possible equalization of the NLI by a single cycle. Trials with 2, 3 and 4 cycles and different phases of the profile gave similar penalties, within 0.1 dB, to those shown in tables 2 and 3. The EDFAs were assumed to have a constant noise figure across all DWDM channels. While the EDFA gain ripple has considerable structure the noise figure depends on the population inversion of Erbium ions and the ratio of absorption to emission cross section. The former is a constant while the latter is a smooth function following the

Parameter	Value	Units
Span length (L)	80	km
Attenuation coefficient (α)	0.22	dB·km^{-1}
Group-velocity dispersion (β_2)	-21.3	ps^2·km^{-1}
Dispersion coefficient (D)	16.7	ps·nm^{-1}·km^{-1}
Nonlinear coefficient (γ)	1.3	W^{-1}·km^{-1}
Symbol rate (B)	32	GBd
DWDM grid spacing	50	GHz
Number DWDM channels (W)	80	
EDFA noise figure (NF)	5	dB

Table 6. List of simulation parameters assumed.

McCumber relation [21]. A small variation in noise figure across the transmission band is expected and the effects of this are left for further study.

For a light path of N spans supporting W, DWDM channels we define $P_{w,s}$ as the signal power launched into span s for channel w. The signal power after a single span is given by

$$P_{w,s+1} = P_{w,s} 10^{-\frac{\alpha L}{10}} 10^{\frac{\alpha L + \Delta G_w}{10}} \tag{17}$$

and the ASE noise is given by

$$a_{w,s} = 10^{\frac{NF}{10}} h\nu 10^{\frac{\alpha L + \Delta G_w}{10}} B \tag{18}$$

where NF is the amplifier noise figure and B is the receiver matched filter bandwidth equal to the symbol rate. The ratio of ASE noise generated in span s to the output signal power is:

$$\frac{1}{SNR^{ASE}_{w,s}} = \frac{a_{w,s}}{P_{w,s+1}} = \frac{10^{\frac{NF}{10}} h\nu 10^{\frac{\alpha L}{10}} B}{P_{w,s}} \tag{19}$$

As the ASE noise and output signal power both depend on ΔG the gain ripple has no effect on $SNR^{ASE}_{w,s}$ for a single span. For multi-span transmission the gain ripple affects the launch power into subsequent spans changing the ratio of ASE noise to signal power generated for those spans. The accumulation of ASE noise through the, N, spans leads to a linear contribution to the overall SNR, SNR^{ASE} given by

$$\frac{1}{SNR^{ASE}_{w}} = 10^{\frac{NF}{10}} h\nu 10^{\frac{\alpha L}{10}} B \sum_{s \in 1 \ldots N} \frac{1}{P_{w,s}}. \tag{20}$$

We break the nonlinear noise term into XCI and SCI separately. For the XCI the nonlinear noise for each span is assumed to add incoherently leading to

$$\frac{1}{SNR^{XCI}_{w}} = \sum_{s \in 1 \ldots N_s} \sum_{w' \in 1 \ldots W \setminus w} X_{w,w'} P^2_{w',s} \tag{21}$$

where $X_{w,w'}$ has been defined in [equations (6) and (7) 22] and describes the nonlinear interference caused by channel w' on channel w. The SCI nonlinear noise term was accumulated coherently such that

$$\frac{1}{SNR^{SCI}_{w}} = X_{w,w} \sum_{s \in 1 \ldots N_s} \sum_{s' \in 1 \ldots N} P_{w,s} E_{s,s'} P_{w,s'} \tag{22}$$

where the matrix E describes the coherence addition factor, related to the correlation between the SCI generated in any two spans. $E_{s,s} = 1$ while $E_{s,s'} < 1 \quad \forall \quad s \neq s'$ and $E_{s,s'} \to 0$ as $|s - s'| \to \infty$. Following [equations (17)–(19) 20] we can find,

$$E_{s,s'} = \frac{\int\int\int q(f_1, f_2, f) r(s, s', f_1, f_2, f) df_1 df_2 df}{\int\int\int q(f_1, f_2, f) df_1 df_2 df} \tag{23}$$

where

$$q(f_1, f_2, f) = g(f_1) g(f_2) g(f_1 + f_2 - f) g(f) \rho(f_1, f_2, f)$$

and

$$r(s, s', f_1, f_2, f) = \cos\left[|s - s'| 4\pi^2 \beta_2 L (f_1 - f)(f_2 - f)\right]$$

where $g(.)$ represents the signal spectral shape a rectangular function with full width R and height 1, $\rho(f_1, f_2, f)$ is given in [20] equation (2), β_2 is the fibre dispersion coefficient and L the span length. $E_{s,s'}$ is a function of $|s - s'|$ and in this work for $|s - s'| = 0, 1, 2$ was calculated to be $1, 0.2243, 0.1019$ while for $|s - s'| > 2$ was well approximated by $\dfrac{0.2019}{|s - s'|}$.

The SNR of a signal in channel w, SNR_w is given by the accumulation of ASE, XCI and SCI noise terms as,

$$\frac{1}{SNR_w} = \frac{1}{SNR_w^{ASE}} + \frac{1}{SNR_w^{XCI}} + \frac{1}{SNR_w^{SCI}} \tag{24}$$

For the network capacity simulation the EDFAs were assumed to be ripple free and a spectrally flat constant signal power, P, launched for each channel into each span. The SCI coherent approximation from [23] was used. Under these simplifying assumptions we find the worst case SNR from

$$\frac{1}{SNR} = \frac{N\, a + P_{NLI}}{P} \tag{25}$$

where

$$P_{NLI} = P^3 \left(X_{w,w} N^{1+\epsilon} + N \sum_{w' \in \{1..W \setminus w\}} X_{w,w'} \right) \tag{26}$$

where $w = \left\lceil \frac{W}{2} \right\rceil$ the worst case central channel, N is the number of spans, a is the ASE noise generated in a single span see equation Eq. (18) and ϵ was calculated to be 0.2186.

ACKNOWLEDGMENTS

RJV acknowledges funding from EPSRC and BT through an iCASE studentship. SJS and DJI acknowledge funding through the EPSRC Programme Grant TRANSNET EP/R035342/1.

REFERENCES

1. Y. Pointurier, "Design of low-margin optical networks," IEEE/OSA J. Opt. Commun. Netw. **9**, A9–A17 (2017).
2. D. J. Ives, P. Bayvel, and S. J. Savory, "Routing, modulation, spectrum and launch power assignment to maximize the traffic throughput of a nonlinear optical mesh network," Photonic Netw. Commun. **29**, 244–256 (2015).
3. H. Chin, D. Charlton, A. Borowiec, M. Reimer, C. Laperle, M. O'Sullivan, and S. J. Savory, "Probabilistic design of optical transmission systems," J. Light. Technol. **35**, 931–940 (2017).
4. S. J. Morrison, "The study of variability in engineering design," J. Royal Stat. Soc. Ser. C (Applied Stat.) **6**, 133–138 (1957).
5. A. Splett, C. Kurzke, and K. Petermann, "Ultimate transmission capacity of amplified optical fiber communication systems taking into account fiber nonlinearities," in *Proc. ECOC 1993,* , vol. 2 (1993), pp. 41–44.
6. Y. Sun, A. K. Srivastava, J. Zhou, and J. W. Sulhoff, "Optical fiber amplifiers for WDM optical networks," Bell Labs Tech. J. **4**, 187–206 (1999).
7. E. de A. Barboza, M. J. da Silva, L. D. Coelho, C. J. A. Bastos-Filho, and J. F. Martins Filho, "Amplifier Adaptive Control of Operating Point Considering Non-Linear Interference," IEEE Photonics Technol. Lett. **30**, 573–576 (2018).
8. F. Forghieri, R. W. Tkach, and D. Favin, "Simple model of optical amplifier chains to evaluate penalties in WDM systems," J. Light. Technol. **16**, 1570–1576 (1998).
9. I. Roberts, J. M. Kahn, and D. Boertjes, "Convex Channel Power Optimization in Nonlinear WDM Systems Using Gaussian Noise Model," J. Light. Technol. **34**, 3212–3222 (2016).
10. I. Roberts, J. M. Kahn, J. Harley, and D. W. Boertjes, "Channel Power Optimization of WDM Systems Following Gaussian Noise Nonlinearity Model in Presence of Stimulated Raman Scattering," J. Light. Technol. **35**, 5237–5249 (2017).
11. D. Semrau, R. I. Killey, and P. Bayvel, "The Gaussian Noise Model in the Presence of Inter-Channel Stimulated Raman Scattering," J. Light. Technol. **36**, 3046–3055 (2018).
12. M. Cantono, D. Pilori, A. Ferrari, C. Catanese, J. Thouras, J. L. Auge, and V. Curri, "On the Interplay of Nonlinear Interference Generation with Stimulated Raman Scattering for QoT Estimation," J. Light. Technol. **36**, 3131–3141 (2018).
13. C. E. Shannon, "A mathematical theory of communication," Bell Syst. Tech. J. **27**, 379–423 (1948).
14. J. M. Simmons, *Optical Network Design and Planning* (Springer, 2014).
15. I. Chlamtac, A. Ganz, and G. Karmi, "Purely optical networks for terabit communication," in *IEEE INFOCOM '89, Proc. 8th Ann. Conf. IEEE Comp. Commun. Soc.*, (1989), pp. 887–896 vol.3.
16. R. J. Vincent, D. J. Ives, and S. J. Savory, "Estimating network throughput with an adaptive routing and wavelength assignment algorithm," in *Opt. Fiber Commun. Conf.*, (Optical Society of America, 2018), p. M2E.2.
17. R. J. Vincent, D. J. Ives, and S. J. Savory, "Scalable capacity estimation for nonlinear elastic all-optical core networks," Under review.
18. "Network Aspects (NA); Availability performance of path elements of international digital paths EN 300 416 v 1.2.1," (ETSI, 1998).
19. A. Betker, I. Gamrath, D. Kosiankowski, C. Lange, H. Lehmann, F. Pfeuffer, F. Simon, and A. Werner, "Comprehensive topology and traffic model of a nationwide telecommunication network," J. Opt. Commun. Netw. **6**, 1038–1047 (2014).
20. P. Poggiolini, "The GN Model of Non-Linear Propagation in Uncompensated Coherent Optical Systems," J. Light. Technol. **30**, 3857–3879 (2012).
21. W. J. Miniscalco and R. S. Quimby, "General procedure for the analysis of Er^{3+} cross sections," Opt. Lett. **16**, 258 (1991).
22. D. Ives, P. Bayvel, and S. Savory, "Adapting Transmitter Power and Modulation Format to Improve Optical Network Performance Utilizing the Gaussian Noise Model of Nonlinear Impairments," J. Light. Technol. **32**, 3485–3494 (2014).
23. G. Bosco, R. Cigliutti, A. Nespola, A. Carena, V. Curri, F. Forghieri, Y. Yamamoto, T. Sasaki, Y. Jiang, and P. Poggiolini, "Experimental investigation of nonlinear interference accumulation in uncompensated links," IEEE Photonics Technol. Lett. **24**, 1230–1232 (2012).